Solid-State Electronics 198 (2022) 108456

Contents lists available at ScienceDirect

Solid State Electronics

journal homepage: www.elsevier.com/locate/sse

Efficient atomistic simulations of lateral heterostructure devices with metal contacts☆,☆☆

Mincheol Shin *, Seonghyeok Jeon, Kanghyun Joo

Korea Advanced Institute of Science and Technology, 291 Daehak-ro, Daejeon, 34141, Republic of Korea

ARTICLE INFO

Keywords:
Modeling and simulations
Lateral heterostructure
Mode-space transformation
Density functional theory
Non-equilibrium Green's function
Schottky contact

ABSTRACT

In this work we present a highly efficient method to perform quantum transport simulations on atomistic devices with metal contacts. In particular, we consider lateral heterostructures of silicide/semi-conductor/silicide and metal/semi-metal/metal which are constructed by the first-principles density functional theory method. We show that large-sized heterostructure Hamiltonian can be effectively reduced, while not losing the accuracy in a practical sense, enabling highly efficient calculation of the electrical transport properties of the devices based on the non-equilibrium Green's function method.

1. Introduction

As the role of the interfaces, junctions and contacts is increasingly important in ultra-scaled devices, it has become necessary to include them as integral parts of simulated device. Although the empirical tight binding (ETB) method combined with the non-equilibrium Green's function (NEGF) method is the state-of-the-art atomistic device simulation methodology [1,2], it has serious limitations in dealing with heterogeneous structures consisting of different materials. The parameter-free density functional theory (DFT) method which is naturally suited for the problem is therefore called for.

A major obstacle of adopting DFT method in device simulations is the computational burden of handling large-sized DFT Hamiltonian. This must be overcome if the DFT Hamiltonian is to be actively used in realistic device simulations in place of ETB. In this regard, the Hamiltonian size reduction method is attractive because the computational time and resources can be reduced by a few orders of magnitude, while the errors in the charge density and current are kept within a few percents or less. The reduction method for DFT Hamiltonian has been developed for homogeneous structures [3,4] and recently extended to treat heterostructures [5]. In this work, we further extend the application of the latter method to heterogeneous structures with metallic contacts, paving the way for realistic simulations of future generation logic and memory devices at the atomistic scale.

2. Hamiltonian size reduction for lateral heterostructures

A generic lateral heterostructure device consisting of three different materials, represented by unit cells A, B, and C, is shown in Fig. 1-(a). Between two materials there are junction cells $J_1, \ldots, J_{p(q)}$ that may show spatially transient behavior in terms of the atom species and their positions. Our goal is to reduce the Hamiltonian of each cell and reconstruct the same device with the effective Hamiltonians as shown in Fig. 1-(d).

The basic idea of the Hamiltonian size reduction method is to unitarily transform the full Hamiltonian to a smaller sized matrix within an energy window of interest where the charge transport takes place. This is possible by constructing a transformation matrix U consisting of a few selected Bloch states within the energy window which is usually a few tenths of eV from the band edges. The so-called mode-space transformation has been developed for various Hamiltonians such as effective mass theory [6,7], k·p method [8], TB [9–11], pseudo-potential [12,13], and DFT Hamiltonians [3,14]. For TB and atomic-orbital based DFT Hamiltonians, it is necessary to remove unphysical states arising from the transformation [3,9].

For heterostructures, however, it is not feasible to obtain the Bloch states of each component cell as some cells like junction cells cannot be repeated periodically. Instead, we form a supercell that consists of minimal number of cells with which the device in Fig. 1-(a) can be constructed. See Fig. 1-(b). In the figure, cells labeled as B_f are needed in addition, which are the buffer cells in case the supercell is terminated

☆ This work was supported in part by the National Research Foundation of Korea (NRF) funded by the Ministry of Science and ICT under Grant NRF-2021R1H1A2094183. and in part by Samsung Research Funding & Incubation Center of Samsung Electronics under Project Number SRFC-IT1901-11.
☆☆ The review of this paper was arranged by Francisco Gamiz.
* Corresponding author.
E-mail address: mshin@kaist.ac.kr (M. Shin).

https://doi.org/10.1016/j.sse.2022.108456

Available online 23 September 2022

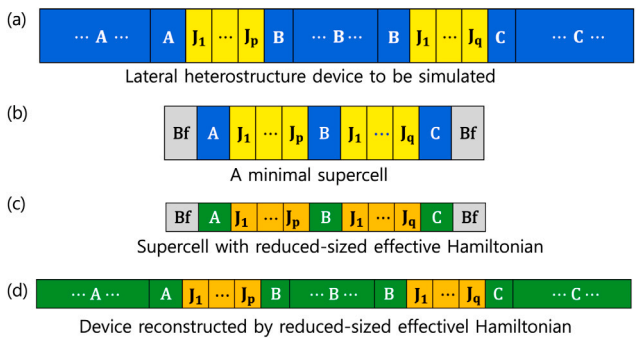

Fig. 1. (a) Schematic of a lateral heterostructure device consisting of three materials. Cells A, B, and C are the unit cells and $J_1, .., J_{p(q)}$ are the junction cells. (b) A supercell consisting of minimal number of cells. Cells B_f are the buffer cells. In (c) and (d), each cell is reduced in size in its Hamiltonian.

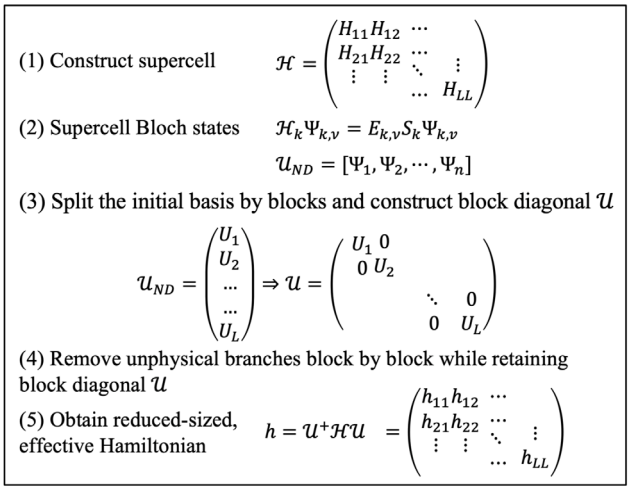

Fig. 2. Steps for lateral heterostructure device simulations by the Hamiltonian reduction method.

with vacuum or junction cells in case the supercell itself is repeated periodically. We relax the supercell by the DFT method and extract its Hamiltonian, which is a block matrix with L block elements, where L is the number of cells in the supercell. For example, for the supercell of Fig. 1(b), $L = p + q + 3$ (for three unit cells of A, B, and C) + 2 (for two buffer cells).

We solve the $E - k$ electronic band structure problem for the supercell and obtain its Bloch states $\Psi_{k,\nu}$ where k is the usual wave vector and ν is the subband index. With the obtained Bloch states, we form a matrix $U_{\mathrm{ND}} = [\Psi_1, \ldots, \Psi_i, \ldots, \Psi_n]$, where index i denotes (k, ν) and n is the number of selected supercell Bloch states. U_{ND} is the matrix of size $N_T \times n$ where N_T is the size of the supercell Hamiltonian $\mathcal{H}$, given as $N_T = \sum_{b=1}^{L} N_b$ where N_b is the Hamiltonian size of block b. See step (2) of Fig. 2. We then make an initial diagonal matrix U by placing sub-blocks of U_{ND} to the diagonal entries (step (3) of Fig. 2). Next we systematically remove the unphysical states on a block-by-block basis so as to retain the block diagonal form of U [5]. If all the unphysical branches are cleared, we obtain the effective supercell each block of which is reduced in its Hamiltonian size as shown in Fig. 1-(c). Finally we reconstruct the heterostructure device with the effective heterostructure Hamiltonian as shown in Fig. 1-(d), and apply the NEGF method to calculate the charge density and current.

The convergence behavior of our Hamiltonian reduction method for hetero-structure is no different from that for homo-structure. Namely, for both the homo- and hetero-structures, the convergence behavior majorly depends on the choice of initial Bloch states. However, the systematic selection scheme as outlined in Ref. [3] is usually efficient. With our approach, devices consisting of a few thousand atoms (for example, nanowire structure with diameter of 3 nm and length of 20 nm) can be handled by utilizing a small cluster computer of several nodes. In this work, however, smaller-sized devices are considered because full-Hamiltonian solutions, which limit the computing resources, are to be compared with the reduced-sized-Hamiltonian solutions as will be shown in Section 3.

3. Applications to structures with metallic regions

In our previous work [5], we have demonstrated the effectiveness and accuracy of the Hamiltonian size reduction method described in the previous Section by taking the four examples devices of GaSb/InAs tunnel field effect transistors (FETs), MoTe2/SnS2 bilayer vertical FETs, InAs nanowire FETs with a defect, and Si nanowire FETs with rough surfaces. The Hamiltonian size was reduced to around 5% of the original full-Hamiltonian size without losing the accuracy of the calculated transmission and local density of states [5]. All the four devices had semi-conductors in their source, channel and drain regions so naturally the energy window of interest where most of charge transport takes place was taken to be a few tenths of eV from the conduction band minima or valence band maxima.

In this work we applied the Hamiltonian reduction method to the structure which includes metallic region(s). Firstly, NiSi/Si/NiSi Schottky barrier structure in the nanowire geometry (see Fig. 3) is considered where NiSi silicide is assumed a crystal phase and shows metallic behavior. The supercell is 6.1 nm long and 1.0 nm in diameter and consists of 10 blocks of total 533 atoms, where block 1 and block 6 are NiSi and Si unit cells, respectively, and blocks 3, 4 and 8, 9 are the junction cells. Blocks 2, 10, and 5, 7 are the junction cells according to Fig. 1-(a) but may as well be called the buffer cells as they are only slightly different from the NiSi or Si unit cells. The periodic boundary condition was applied to the supercell. We used the SIESTA package [15] to relax the supercell until the maximum force on any of the atoms becomes less than 0.04 eV/Å. A standard GGA-PBE functional [16] with the DZP pseudoatomic orbital basis set was used for the DFT method. In the junction cells, the atoms are seen unorderly positioned as the stress due to the lattice mismatch is applied in the regions. Table in Fig. 3-(b) shows the result of the heterostructure Hamiltonian reduction in the energy window of −3.0 eV to −1.5 eV. The Hamiltonian size is reduced to about 15% of the original size. As expected, due to the effect of the metallic region, the reduction rate is not as high as in the cases of all-semiconductor structures.

Fig. 4-(a) shows the local density of states (LDOS) profile near the left junction. The Si conduction band edge (E_c) is at −2.35 eV and the Schottky barrier height is 1.37 eV, which is quite large due to the confinement effect of ultra-scaled nanowire structure. In the figure, LDOS of the junction region is distinctively lower compared to that of the metallic NiSi and may represent the interface states at the NiSi/Si junction. This feature is very well reproduced by the reduced-sized effective Hamiltonian, as seen in Fig. 4-(b) where LDOS is evaluated at a cross-section in the junction region. Since LDOS is faithfully reproduced by the reduced-sized Hamiltonian, a NEGF-Poisson self-consistent calculation can be readily performed. The full transport calculation results will be published elsewhere.

In Fig. 4-(c), the transmission through the device structure of Fig. 1-(a) with the source and drain regions constructed by repeating cell 1 indefinitely is evaluated. Again, the transmission evaluated by using the effective Hamiltonian agrees quite well with that evaluated by using the much larger-sized full Hamiltonians, while the computation speed is more than 2 orders faster.

Fig. 5-(a) shows TiN/Sb/TiN heterostructure where a-few-layer Sb semi-metal is contacted with TiN metal, with a potential application as a next-generation phase-change memory in mind. The supercell in the thin film geometry is 7.5 nm long, 1.0 nm thick and periodic

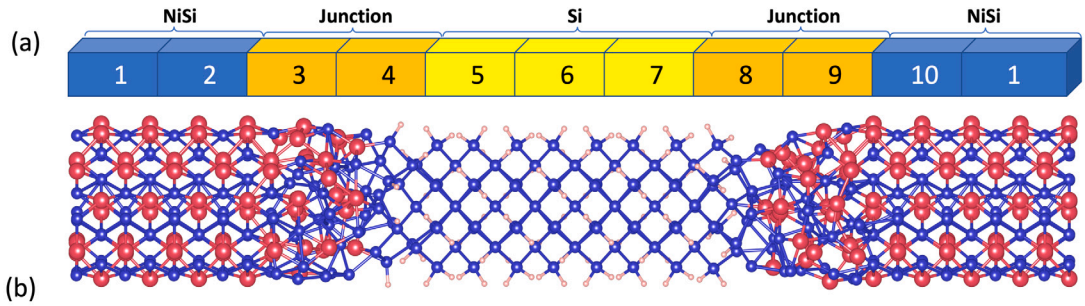

Cell	1	2	3	4	5	6	7	8	9	10	1
N_{atom}	64	64	64	43	41	41	41	46	65	64	64
N_b	896	896	894	433	373	373	373	532	911	896	896
n_b	124	124	99	79	57	57	57	82	99	109	124

Fig. 3. (a) NiSi/Si/NiSi supercell consisting of 10 blocks. The supercell in the nanowire geometry is 6.1 nm long and 1.0 nm in diameter and repeated periodically lengthwise. Red and blue balls represent Ni and Si atoms, respectively, and small empty balls hydrogen passivation atoms. (b) Table shows number of atoms (N_{atom}), size of full Hamiltonian (N_b) and size of the reduced Hamiltonian (n_b) of each block. (For interpretation of the references to color in this figure legend, the reader is referred to the web version of this article.)

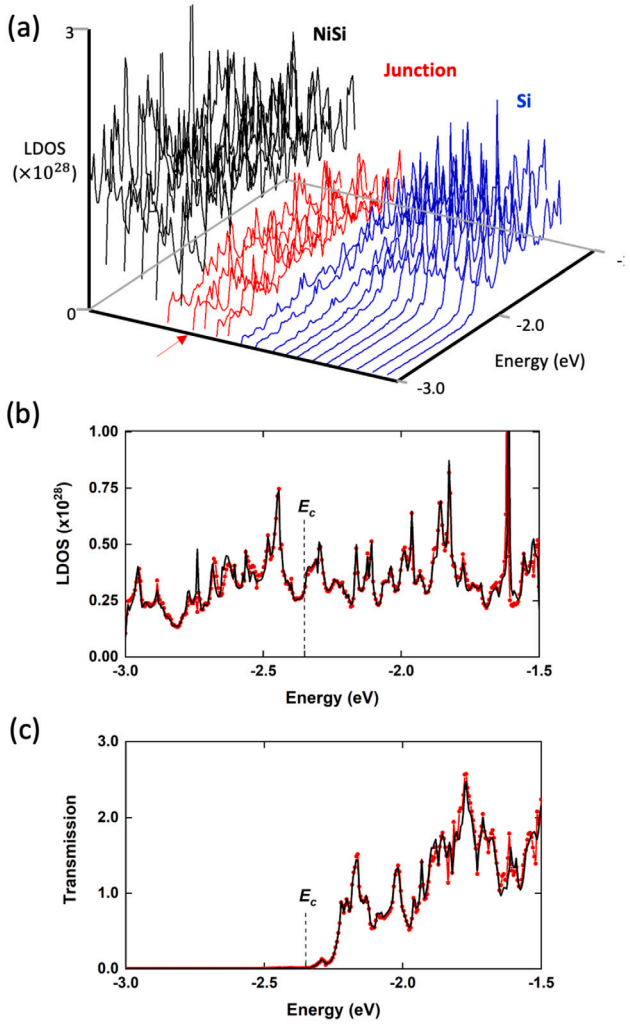

Fig. 4. (a) LDOS profile around the left junction of the NiSi/Si/NiSi structure of Fig. 3-(a). The LDOS in the junction region are highlighted by the red color. The unit of LDOS is $[\text{eV m}^3]^{-1}$. (b) LDOS at the cross-section indicated by the arrow in (a). (c) Transmission through the device structure. In (b) and (c), black lines and red dots with lines represent the results calculated by using the full Hamiltonian and reduced-sized effective Hamiltonian, respectively. (For interpretation of the references to color in this figure legend, the reader is referred to the web version of this article.)

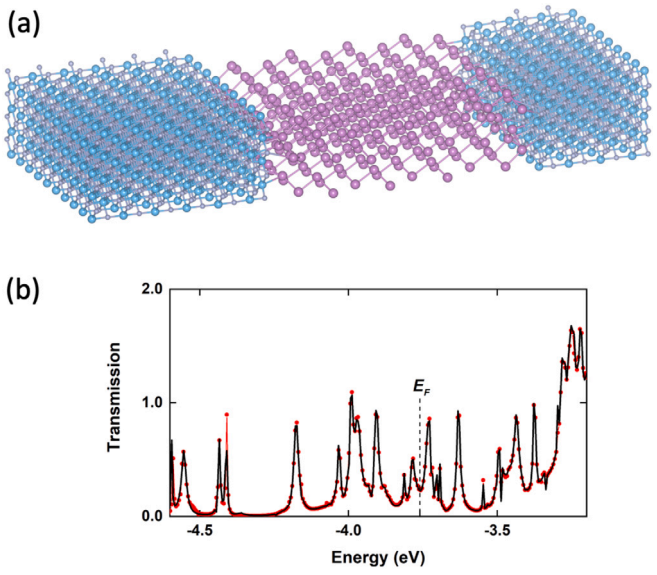

Fig. 5. (a) TiN/Sb/TiN structure in the thin film geometry. The supercell is 7.5 nm long, 1.0 nm thick and periodic in the perpendicular direction. (b) Transmission calculated by the full Hamiltonian (black lines) and reduced-sized Hamiltonian (red dots with thin lines). The Fermi energy of the entire structure (E_F) is −3.67 eV as indicated. (For interpretation of the references to color in this figure legend, the reader is referred to the web version of this article.)

in the perpendicular direction. The supercell with total of 580 atoms are similarly handled to yield the reduced-sized effective Hamiltonian, which excellently reproduces the transmission in the energy window of 1.5 eV wide as shown in Fig. 5-(b).

4. Conclusions

In this work, we have successfully applied the Hamiltonian reduction method to laterally heterostructured devices of NiSi/Si/NiSi and TiN/Sb/TiN. We have shown that computationally demanding task due to the involvement of metal contacts can be handled efficiently, paving the way for large-scale atomistic simulations of practically relevant contact problems.

CRediT authorship contribution statement

Mincheol Shin: Conceptualization of this study, Methodology, Software. **Seonghyeok Jeon:** DFT relaxation of atomic structures and Hamiltonian matrix extraction. Contributed to calculation and analysis of LDOS and transmission.. **Kanghyun Joo:** DFT relaxation of atomic structures and Hamiltonian matrix extraction..

Declaration of competing interest

The authors declare that they have no known competing financial interests or personal relationships that could have appeared to influence the work reported in this paper.

Data availability

Data will be made available on request.

References

[1] Fonseca JE, Kubis T, Povolotskyi M, Novakovic B, Ajoy A, Hegde G, Ilatikhameneh H, Jiang Z, Sengupta P, Tan Y, Klimeck G. Efficient and realistic device modeling from atomic detail to the nanoscale. J Comput Electron 2013;12(4):592–600.

[2] Luisier M, Schenk A, Fichtner W, Klimeck G. Atomistic simulation of nanowires in the $sp^3d^5s^*$ tight-binding formalism: From boundary conditions to strain calculations. Phys Rev B 2006;74:205323.

[3] Shin M, Jeong WJ, Lee J. Density functional theory based simulations of silicon nanowire field effect transistors. J Appl Phys 2016;119(15):154505.

[4] Shin M, Jung H-E, Jung S. First-principles based quantum transport simulations of nanoscale field effect transistors. In: 2017 IEEE international electron devices meeting (IEDM). 2017, p. 35.2.1–4.

[5] Shin M. Hetero-structure mode space method for efficient device simulations. J Appl Phys 2021;130(10):104303.

[6] Venugopal R, Ren Z, Datta S, Lundstrom MS, Jovanovic D. Simulating quantum transport in nanoscale transistors: Real versus mode-space approaches. J Appl Phys 2002;92(7):3730–9.

[7] Shin M. Efficient simulation of silicon nanowire field effect transistors and their scaling behavior. J Appl Phys 2007;101(2):024510.

[8] Shin M. Full-quantum simulation of hole transport and band-to-band tunneling in nanowires using the k·p method. J Appl Phys 2009;106(5):054505.

[9] Mil'nikov G, Mori N, Kamakura Y. Equivalent transport models in atomistic quantum wires. Phys Rev B 2012;85(3):035317.

[10] Jeong WJ, Seo J, Shin M. Efficient TB-NEGF simulations of ultra-thin body tunnel FETs. In: 2016 international conference on simulation of semiconductor processes and devices (SISPAD). 2016, p. 81–4.

[11] Afzalian A, Akhoundi E, Gaddemane G, Duflou R, Houssa M. Advanced DFT–NEGF transport techniques for novel 2-D material and device exploration including HfS2/WSe2 van der Waals heterojunction TFET and WTe2/WS2 metal/semiconductor contact. IEEE Trans Electron Devices 2021;68(11):5372–9.

[12] Van de Put ML, Fischetti MV, Vandenberghe WG. Scalable atomistic simulations of quantum electron transport using empirical pseudopotentials. Comput Phys Comm 2019;244:156–69.

[13] Pala MG, Esseni D. Quantum transport models based on NEGF and empirical pseudopotentials for accurate modeling of nanoscale electron devices. J Appl Phys 2019;126(5):055703.

[14] Pala MG, Giannozzi P, Esseni D. Unit cell restricted Bloch functions basis for first-principle transport models: Theory and application. Phys Rev B 2020;102(4):045410.

[15] Soler JM, Artacho E, Gale JD, García A, Junquera J, Ordejón P, Sánchez-Portal D. The SIESTA method for ab initio order-N materials simulation. J Phys: Condens Matter 2002;14(11):2745.

[16] Perdew JP, Burke K, Ernzerhof M. Generalized gradient approximation made simple. Phys Rev Lett 1996;77:3865–8.